

Structural characterisation of metal complexes containing 1-[(4-methylphenyl)sulfonamido]-2-[(2-pyridylmethylene)amino]benzene

Antonio Sousa,^{*a} Manuel R. Bermejo,^{*a} Matilde Fondo,^a Ana García-Deibe,^a Antonio Sousa-Pedrares^a and Oscar Piro^b

^a Departamento de Química Inorgánica, Facultad de Química, Universidad de Santiago, E-15706 Santiago de Compostela, Spain. E-mail: qiansoal@uscmail.usc.es

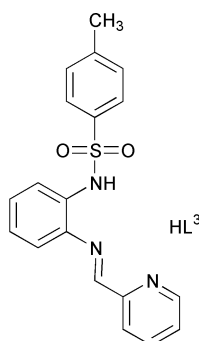
^b Departamento de Física, Facultad de Ciencias Exactas, Universidad de La Plata, C.C. 67-1900, La Plata, Argentina

Received (in Montpellier, France) 6th November 2000, Accepted 26th January 2001

First published as an Advance Article on the web 19th March 2001

The interaction of 2-pyridinecarboxaldehyde with *N*-tosyl-1,2-diaminobenzene leads to the isolation of two different products, {3-[ethoxy(2-pyridyl)methyl]-1-[(4-methylphenyl)sulfonyl]-2-(2-pyridyl)-2,3-dihydro-1*H*-benzo[*d*]imidazole}, L¹, and {1-[(4-methylphenyl)sulfonyl]-2-(2-pyridyl)-2,3-dihydro-1*H*-benzo[*d*]imidazole}, L², but not to the expected Schiff base 1-[(4-methylphenyl)sulfonamido]-2-[(2-pyridylmethylene)amino]benzene, HL³. Two kinds of complexes, containing the potentially tridentate and monoanionic [L³][−] as a ligand, were obtained by different routes. ML³(*p*-Tos)(H₂O)_{*n*} complexes (*p*-TosH = *p*-toluenesulfonic acid; M = Co, Cu, Zn; *n* = 1–3) have been isolated by electrolysis of a solution phase composed of L¹ and *p*-toluenesulfonic acid, using metal plates as the anode. Metal complexes of composition ML³₂(H₂O)_{*n*} (M = Mn, Co, Cu, Zn; *n* = 0–2) were obtained by template synthesis from M(acac)₂, 2-pyridinecarboxaldehyde and *N*-tosyl-1,2-diaminobenzene. All these compounds have been characterised by elemental analyses, magnetic measurements, IR, mass spectrometry and, in the case of M = Zn, by ¹H NMR spectroscopy. CuL³(*p*-Tos)(H₂O), **1**, ZnL³(*p*-Tos)(H₂O), **2**, CoL³₂, **3**, CuL³₂, **4** and ZnL³₂ · 2CH₃CN, **5**, were also crystallographically characterised.

Schiff base complexes are considered to be among the most important stereochemical models in main group and transition metal co-ordination chemistry due to their preparative accessibility and structural variety.^{1–3} Our investigations in the area of the imine-based ligands have been mainly centred on the co-ordination chemistry of tetradentate Schiff bases containing N,O-donors.⁴ More recently, we have turned our attention to the study of asymmetric tridentate Schiff bases with N-donors and we found that, in contrast to the general pattern, the Schiff base 1-[(4-methylphenyl)sulfonamido]-2-[(2-pyridylmethylene)amino]benzene, HL³, cannot be isolated by direct condensation of the corresponding amine and aldehyde.⁵ In spite of this, a nickel complex containing [L³][−] was obtained and crystallographically characterised.⁵ As a continuation of this work, we extended our studies to other metals. Herein, we report the synthesis and characterisation of Mn, Co, Cu and Zn complexes containing the monoanion of the asymmetric and potentially tridentate (N₃) Schiff base HL³ as a ligand.



Results and discussion

Syntheses

Previous studies⁵ have shown that the direct interaction of *N*-tosyl-1,2-diaminobenzene and 2-pyridinecarboxaldehyde does not produce the Schiff base HL³ but two different organic products (L¹ and L²), depending on the reaction conditions (see Scheme 1).

Thus, we tried to obtain metallic compounds of L¹ via an electrochemical synthetic route. As the ligand has no acidic hydrogen atoms, it was thought necessary to add an acid to the electrolysis phase, in order to obtain M(II) complexes containing L¹. The chosen acid was *p*-toluenesulfonic acid. The reaction was performed in an electrochemical cell that can be summarised as follows:



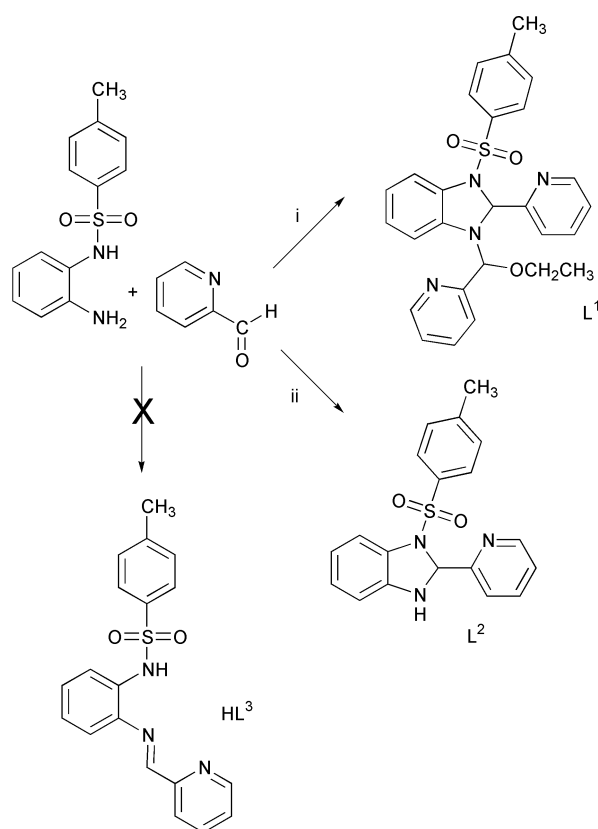
Reactions with Co, Cu and Zn anodes lead to materials of the composition ML³(*p*-Tos)(H₂O)_{*n*} (*n* = 1–3). Crystals of ML³(*p*-Tos)(H₂O) (M = Cu, Zn), suitable for X-ray diffraction studies, were obtained. A manganese anode yields the insoluble Mn(*p*-Tos)₂(H₂O)₆ compound [see Scheme 2(a)]. All these complexes seem to be stable in the solid state and no changes in aspect and/or colour were observed.

These data suggest, once again,⁵ that the ligand L¹ is unstable in solution, rearranging to HL³. Besides, it should be noted that complexes of composition ML³(*p*-Tos)(H₂O)_{*n*} cannot survive for a long time in solution, as they give rise to a series of reactions that, in the end, lead to the formation of more stable products, such as ML³₂(H₂O)_{*n*} and/or M(*p*-Tos)₂(H₂O)_{*n*}. Thus, the reported complex⁶ Co(*p*-Tos)₂(H₂O)₆ is obtained when CoL³(*p*-Tos)(H₂O)₃ is recrystallised in acetoni-

trile (see Experimental). However, recrystallisation of $\text{ZnL}^3(p\text{-Tos})(\text{H}_2\text{O})_2$ in DMSO leads to $\text{ZnL}^3_2(\text{H}_2\text{O})$, which was also characterised by X-ray diffraction. This reorganisation is also supported by the ^1H NMR spectrum of $\text{ZnL}^3(p\text{-Tos})(\text{H}_2\text{O})_2$ in DMSO. The spectrum shows a great number of signals that could not be fully assigned, as discussed below. However, it can be deduced from it that there is a mixture of products and some peaks are typical of the compound ZnL^3_2 .

Due to the tendency of L^1 to reorganise to give HL^3 and to the low stability of $\text{ML}^3(p\text{-Tos})(\text{H}_2\text{O})_n$ complexes in solution, we focussed our efforts on the isolation of compounds of composition $\text{ML}^3_2(\text{H}_2\text{O})_n$. Many attempts were made until a general and reproducible method was achieved (see Scheme 2).

First of all, it was thought that if L^1 can reorganise in the presence of stoichiometric quantities of $p\text{-TosH}$, maybe it was enough to use traces of this acid to obtain the products $\text{ML}^3_2(\text{H}_2\text{O})_n$. The electrochemical interaction of the metal anode with L^1 in acetonitrile in the presence of traces of $p\text{-TosH}$ [Scheme 2(b)] produces materials of unknown nature in all cases, maybe due to the formation of mixtures. A second electrochemical procedure, using L^2 [Scheme 2(c)], was only satisfactory for the isolation of $\text{ZnL}^3_2(\text{H}_2\text{O})$.



Scheme 1 Reaction conditions: (i) absolute ethanol (99%), stir 5 h, RT; (ii) ethanol (96%), stir 5 h, RT or methanol, ethanol (96%) or chloroform, stir 3 h, reflux.

Table 1 Analytical and some selected data for the complexes

Complex	Colour	m.p./°C	Elemental analysis ^a				ESMS ^b	μ/BM
			%C	%H	%N	%S		
$\text{CoL}^3(p\text{-Tos})(\text{H}_2\text{O})_3$	Garnet	99–101	49.5(49.2)	4.1(4.6)	6.4(6.6)	10.1(10.1)	581	3.8
$\text{CuL}^3(p\text{-Tos})(\text{H}_2\text{O})_3$	Dark brown	136–8	49.1(48.9)	4.3(4.5)	7.3(6.6)	10.1(10.0)	584–586	2.1
$\text{ZnL}^3(p\text{-Tos})(\text{H}_2\text{O})_2$	Yellow	283	50.6(50.1)	3.7(4.5)	6.8(6.7)	9.8(10.3)	585–588	—
$\text{MnL}^3_2(\text{H}_2\text{O})$	Brown	282–4	58.6(59.0)	4.3(4.4)	11.0(10.9)	7.9(8.3)	756–757	5.8
CoL^3_2	Dark brown	> 350	59.8(60.2)	3.8(4.0)	11.1(11.0)	6.9(8.5)	759–762	4.1
CuL^3_2	Dark red	221–3	59.2(59.7)	4.2(4.2)	11.0(11.0)	7.1(8.4)	764–766	1.9
$\text{ZnL}^3_2(\text{H}_2\text{O})$	Orange	291–2	58.1(58.2)	4.1(4.3)	10.6(10.7)	8.8(8.2)	765–768	—

^a Found (calc.). ^b Peaks corresponding to $[\text{ML}^3(p\text{-TosH})]^+$ or $[\text{ML}^3_2]^+$.

In a new attempt, electrochemical template synthesis from the metal, *N*-tosyl-1,2-diaminobenzene and 2-pyridinecarboxaldehyde in stoichiometric quantities was performed [Scheme 2(d)]. It was thought that the interaction of the amine and aldehyde over a metal centre during the electrolysis would favour the condensation reaction and the expected complexes would be formed. This new method only allows the isolation of CoL^3_2 . The products obtained in the other cases could not be satisfactorily characterised.

These experiments seem to indicate that the ligands are not stable under the conditions of the electrochemical syntheses. Thus, a chemical procedure involving chemical template synthesis from $\text{M}(\text{acac})_2$, *N*-tosyl-1,2-diaminobenzene and 2-pyridinecarboxaldehyde was tried [Scheme 2(e)]. This method proved to be an easy and general way of isolating the desired complexes in good yield (Table 1).

All $\text{ML}^3_2(\text{H}_2\text{O})_n$ complexes are stable in the solid state, melting without decomposition. Furthermore, the complexes seem to be stable in solution and no rearrangement and/or decomposition processes were observed.

X-Ray crystallography

Crystal structure of $\text{CuL}^3(p\text{-Tos})(\text{H}_2\text{O})$, **1 and $\text{ZnL}^3(p\text{-Tos})(\text{H}_2\text{O})$, **2**.** The crystal structures of **1** and **2** are shown in Fig. 1 and 2, respectively. Experimental details are shown in Table 2 and the main bond distances and angles are displayed in Table 3.

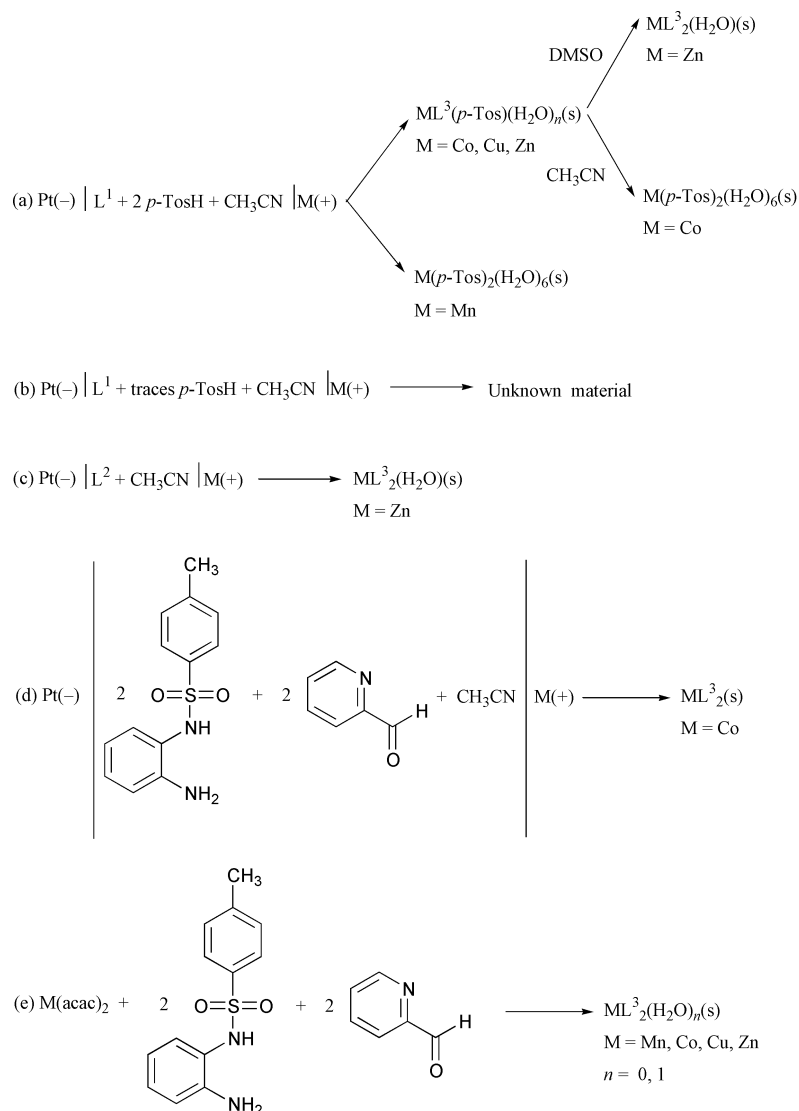
Both compounds consist of discrete $\text{ML}^3(p\text{-Tos})(\text{H}_2\text{O})$ molecules. In complex **2**, four carbon atoms [C(72), C(73), C(75), C(76)] of the aromatic ring and one oxygen atom [O(72)] of the tosylate group are disordered over two sites, with partial occupancies of about 0.65 : 0.35 and 0.87 : 0.13, respectively.

In both complexes the metal atom is in a pentaco-ordinate environment. The geometrical parameter $\tau[\tau = (\beta - \alpha)/60]$, α and β = largest angles between metal and donor atoms] has a value of 0.12 for **1** and 0.32 for **2**, which indicates a geometry closer to square pyramidal ($\tau = 0$) than to trigonal bipyramidal ($\tau = 1$) in both cases.⁷ Thus, the monoanionic tridentate Schiff base and the water molecule fill the basal positions, with the $p\text{-Tos}^-$ ligand occupying the apex.

All the Cu–N bond distances are in the range expected^{8–13} and do not merit further consideration. The Zn–N_{amide} and Zn–N_{imine} distances are in-between those found for tetrahedral^{14–15} and octahedral⁸ compounds with N-donor Schiff bases, as expected. The Zn–N_{pyridine} bond [2.188(8) Å] is longer than those found in five-co-ordinate complexes,¹⁶ but similar¹⁷ [2.181(7) Å] or shorter^{18–19} [2.213(7) Å, 2.251(4) Å] than those reported for seven-co-ordinate compounds containing terminal Zn–N_{pyridine} bonds.

The M–O(1W) bonds are quite short,^{18–22} in spite of the hydrogen bond interactions that the water molecules generate. However, they are not exceptional. A heptaco-ordinate copper complex has been reported²³ to present a short Cu–OH₂ bond of 1.922(3) Å.

A comparison of both pyramids indicates that the deviation from ideal geometry is higher for the zinc complex, as the τ



Scheme 2 Procedures tried in the isolation of the metal complexes. In the reactants, M always denotes Mn, Co, Cu and Zn.

parameter reveals. This is clearly shown by the angles between the oxygen atom at the apex, the metal atom and the donor set of the basal plane, which range from $93.01(19)$ to $97.6(2)^\circ$ for complex **1** and from $100.6(3)$ to $125.6(3)^\circ$ for **2**. In addition, the four angles subtended at the metal atom by adjacent basal atoms also deviate more from the ideal value of 90° in the case of the zinc complex.

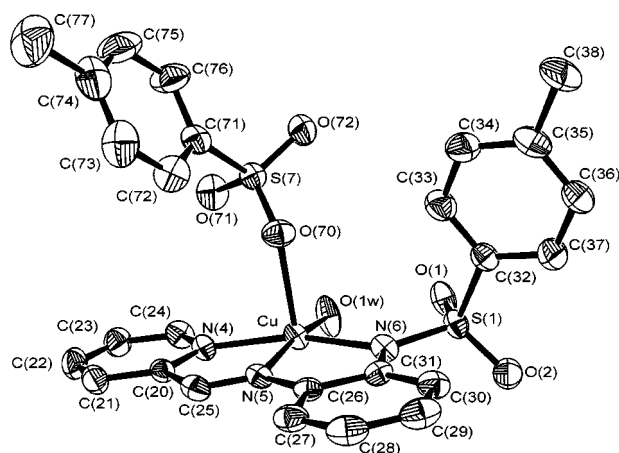


Fig. 1 An ORTEP view of the crystal structure of $\text{CuL}^3(p\text{-Tos})(\text{H}_2\text{O})$, **1**. Ellipsoids are drawn at 50% probability.

The water molecule is involved in similar hydrogen bonds in both cases. One hydrogen atom establishes an intramolecular hydrogen bond with one oxygen atom of the tosyl group belonging to the Schiff base [$\text{O}(1w) \cdots \text{O}(1) = 2.573(7) \text{ \AA}$ for **1** and $\text{O}(1w) \cdots \text{O}(2) = 2.905(11) \text{ \AA}$ for **2**] and the other one with a *p*-toluenesulfonate ligand of a neighbouring unit

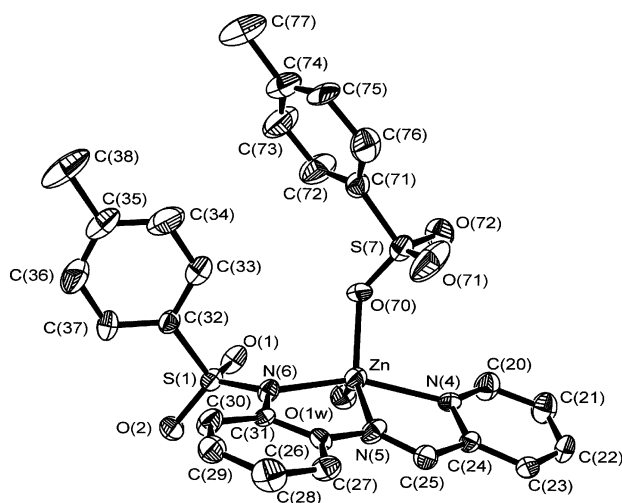


Fig. 2 An ORTEP view of the crystal structure of $\text{ZnL}^3(p\text{-Tos})(\text{H}_2\text{O})$, **2**. Ellipsoids are drawn at 50% probability.

Table 2 Crystal data and structure refinement

	1	2	3	4	5
Empirical formula	C ₂₆ H ₂₆ N ₃ O ₆ CuS ₂	C ₂₆ H ₂₆ N ₃ O ₆ ZnS ₂	C ₃₈ H ₃₂ N ₆ O ₄ CoS ₂	C ₅₇ H ₄₈ N ₉ O ₆ Cu _{1.5} S ₃	C ₄₂ H ₃₈ N ₈ O ₄ ZnS ₂
Formula weight	603.15	604.98	759.75	1146.53	848.29
Crystal system	Triclinic	Triclinic	Monoclinic	Monoclinic	Triclinic
Space group	P $\bar{1}$ (no. 2)	P $\bar{1}$ (no. 2)	P2 ₁ (no. 5)	C2/c	P $\bar{1}$ (no. 2)
a/Å	8.949(3)	9.330(2)	10.780(2)	42.6482(4)	11.372(2)
b/Å	11.071(4)	10.721(4)	15.226(3)	14.7187(2)	11.7922(2)
c/Å	14.162(2)	14.634(3)	11.158(2)	17.705 50(10)	14.668(6)
α /°	77.7390(3)	101.6840(3)	90	90	98.446(18)
β /°	75.0160(5)	103.9560(3)	103.235(4)	112.8850(10)	92.76(2)
γ /°	105.5400(5)	105.5400(5)	90	90	95.033(12)
U/Å ³	1310.3(7)	1311.7(6)	1782.9(6)	10 239.37(18)	1934.4(9)
Z	2	2	2	8	2
μ /mm ⁻¹	1.038	1.141	0.648	0.814	0.798
Reflections collected	6694	4925	9356	23 365	13 600
Independent reflections	6293	4613	5573	11 708	6800
R _{int}	0.0235	0.0711	0.1117	0.0644	0.0895
Final R indices [I > 2 σ (I)]	0.0665	0.0680	0.0573	0.0849	0.0689
R indices (all data)	0.1312	0.2239	0.2280	0.2150	0.1119

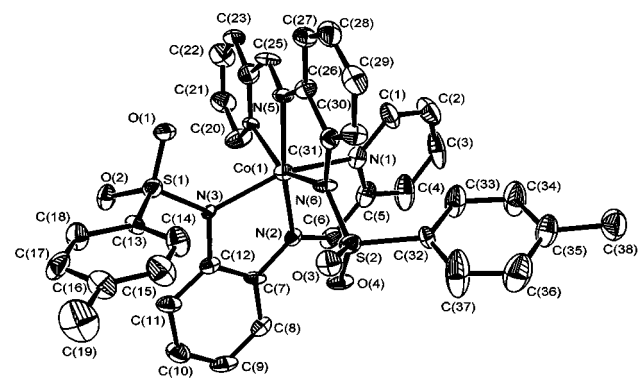
[O(1w)··O(71#)] = 2.630(7) Å for **1** and O(1w)··O(72#) = 2.725(11) Å for **2**. In addition, complex **2** shows weak π -stacking interactions between the basal planes of neighbouring pyramids while this does not seem to occur in **1**.

Crystal structure of CoL₂³, 3. An ORTEP view of the crystal structure of **3** is shown in Fig. 3. Experimental details are presented in Table 2 and the main bond lengths and angles in Table 4.

The complex consists of discrete CoL₂³ molecules. The environment of the cobalt atom is distorted octahedral, with both Schiff bases acting as tridentate N₃ monoanionic donors

Table 3 Selected bond distances (Å) and angles (°) for **1** and **2**

1		2	
Cu–O(1W)	1.939(4)	Zn–O(1W)	1.985(7)
Cu–N(4)	2.000(5)	Zn–N(4)	2.188(8)
Cu–N(5)	1.946(5)	Zn–N(5)	2.081(8)
Cu–N(6)	2.015(5)	Zn–N(6)	2.072(7)
Cu–O(70)	2.263(5)	Zn–O(70)	2.011(7)
O(1W)–Cu–N(4)	96.0(2)	O(1W)–Zn–N(4)	90.8(3)
O(1W)–Cu–N(5)	168.6(2)	O(1W)–Zn–N(5)	133.2(3)
O(1W)–Cu–N(6)	99.14(19)	O(1W)–Zn–N(6)	100.9(3)
O(1W)–Cu–O(70)	97.6(2)	O(1W)–Zn–O(70)	100.6(3)
N(4)–Cu–N(6)	161.5(2)	N(4)–Zn–N(6)	152.5(3)
N(4)–Cu–O(70)	93.01(19)	N(4)–Zn–O(70)	101.3(3)
N(5)–Cu–N(4)	80.9(2)	N(5)–Zn–N(4)	74.9(3)
N(5)–Cu–N(6)	82.2(2)	N(5)–Zn–N(6)	79.1(3)
N(5)–Cu–O(70)	93.49(18)	N(5)–Zn–O(70)	125.6(3)
N(6)–Cu–O(70)	95.44(18)	N(6)–Zn–O(70)	100.9(3)

**Fig. 3** Molecular crystal structure of CoL₂³, **3**. Ellipsoids are drawn at 30% probability.

and adopting a *mer* disposition. The tosyl groups of both ligands are orientated away from each other, maybe in order to avoid steric hindrance. The ligands are not equivalent, in spite of the adopted configuration. However, their bond lengths and angles are very similar.

All the bond distances and angles are unexceptional and compare fairly well with those reported for octahedral cobalt(II) complexes with Schiff bases.^{24,25} The Co–N distances range from 2.065(8) to 2.208(9) Å and follow the sequence Co–N_{pyridine} > Co–N_{amide} > Co–N_{imine}. The distortion of the octahedron is mainly evidenced by the bond angles, which differ significantly from the ideal values of 90 and 180°. This deviation can be attributed to the small bite angles of the Schiff bases, which also force an opening of the perinuclear angles. The structure could be related to that of NiL₂³ · 0.75H₂O, although the symmetry is higher in the case of the cobalt complex.⁵

Crystal structure of CuL₂³, 4. The unit cell contains two distinct molecules, **4A** and **4B**, with different geometries around the central atom. The structures are shown in Fig. 4(a) and (b), respectively, and the main bond lengths and angles are given in Table 5.

Complex **4A** consists of discrete molecules with the copper atom in a pentaco-ordinate environment. One of the Schiff base ligands is tridentate while the second is bidentate, with an unco-ordinated pyridine nitrogen atom [Cu(1)··N(1) = 2.518(7) Å]. This latter distance seems to indicate that the N(1) atom is weakly interacting with the metal atom (secondary intramolecular interaction) but it is too long to be considered a true co-ordinated bond.

The geometrical parameter τ has a value of 0.05. Consequently, the geometry around the copper atom is best described as square pyramidal with a 5% distortion towards

Table 4 Selected bond distances (Å) and angles (°) for **3**

Co(1)–N(1)	2.208(9)	Co(1)–N(4)	2.196(9)
Co(1)–N(2)	2.065(8)	Co(1)–N(5)	2.078(8)
Co(1)–N(3)	2.093(7)	Co(1)–N(6)	2.101(8)
N(2)–Co(1)–N(1)	75.5(4)	N(4)–Co(1)–N(1)	80.7(3)
N(2)–Co(1)–N(3)	78.3(4)	N(5)–Co(1)–N(6)	78.2(3)
N(2)–Co(1)–N(4)	95.9(3)	N(5)–Co(1)–N(1)	93.3(4)
N(2)–Co(1)–N(5)	167.7(4)	N(5)–Co(1)–N(3)	111.7(3)
N(2)–Co(1)–N(6)	107.6(3)	N(5)–Co(1)–N(4)	76.8(4)
N(3)–Co(1)–N(1)	152.0(4)	N(6)–Co(1)–N(1)	94.9(3)
N(3)–Co(1)–N(4)	92.5(3)	N(6)–Co(1)–N(4)	154.3(3)
N(3)–Co(1)–N(6)	102.2(3)		

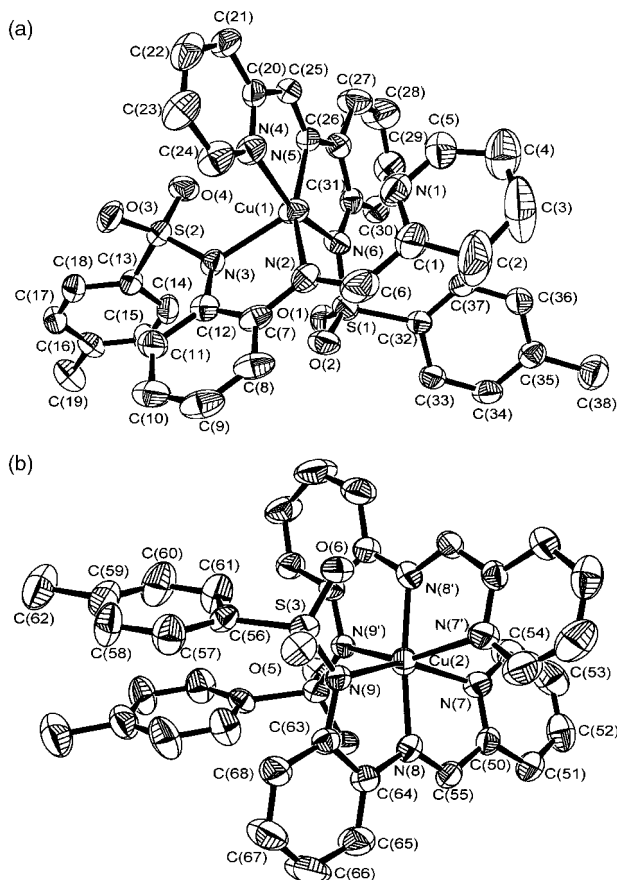


Fig. 4 Molecular crystal structure of $\text{CuL}_3 \cdot 2$, **4**. Ellipsoids are drawn at 30% probability. (a) An ORTEP view of **4A**; (b) an ORTEP view of **4B**.

trigonal bipyramidal. The basal positions are occupied by the tridentate $[\text{L}^3]^-$ ligand and the imine nitrogen atom of the bidentate ligand. The amide nitrogen atom of the latter ligand fills the apical position.

The $\text{Cu}(1)\text{--N}$ distances range from 1.952(5) to 2.170(5) Å. The $\text{Cu}(1)\text{--N}_{\text{imine}}$ and $\text{Cu}(1)\text{--N}_{\text{amide}}$ bonds of the tridentate Schiff base [1.952(5) and 2.026(5) Å, respectively] are significantly shorter than those of the bidentate Schiff base ligand [2.068(6) and 2.170(5) Å]. The shorter distances are closer to the expected values for pentaco-ordinate copper complexes.^{11,12} The longer $\text{Cu}(1)\text{--N}$ distance corresponds to the apical $\text{Cu}(1)\text{--N}(3)$ bond [2.170(5) Å], showing the elongation of the pyramid.

Table 5 Selected bond distances (Å) and angles (°) for **4**

4A		4B	
$\text{Cu}(1)\text{--N}(2)$	2.068(6)	$\text{Cu}(2)\text{--N}(7)$	2.264(6)
$\text{Cu}(1)\text{--N}(3)$	2.170(5)	$\text{Cu}(2)\text{--N}(8)$	1.970(5)
$\text{Cu}(1)\text{--N}(4)$	2.058(6)	$\text{Cu}(2)\text{--N}(9)$	2.178(4)
$\text{Cu}(1)\text{--N}(5)$	1.952(5)		
$\text{Cu}(1)\text{--N}(6)$	2.026(5)		
$\text{N}(2)\text{--Cu}(1)\text{--N}(3)$	77.1(2)	$\text{N}(7)\text{--Cu}(2)\text{--N}(7)$	84.8(3)
$\text{N}(4)\text{--Cu}(1)\text{--N}(2)$	94.9(2)	$\text{N}(8)\text{--Cu}(2)\text{--N}(8')$	173.0(3)
$\text{N}(4)\text{--Cu}(1)\text{--N}(3)$	90.6(2)	$\text{N}(8)\text{--Cu}(2)\text{--N}(9')$	105.87(18)
$\text{N}(5)\text{--Cu}(1)\text{--N}(2)$	157.5(2)	$\text{N}(8)\text{--Cu}(2)\text{--N}(9)$	78.66(18)
$\text{N}(5)\text{--Cu}(1)\text{--N}(3)$	124.5(2)	$\text{N}(8)\text{--Cu}(2)\text{--N}(7)$	76.86(19)
$\text{N}(5)\text{--Cu}(1)\text{--N}(4)$	80.0(2)	$\text{N}(8)\text{--Cu}(2)\text{--N}(7')$	97.90(19)
$\text{N}(5)\text{--Cu}(1)\text{--N}(6)$	80.4(2)	$\text{N}(9)\text{--Cu}(2)\text{--N}(9)$	101.8(2)
$\text{N}(6)\text{--Cu}(1)\text{--N}(2)$	103.3(2)	$\text{N}(9)\text{--Cu}(2)\text{--N}(7)$	154.51(18)
$\text{N}(6)\text{--Cu}(1)\text{--N}(3)$	100.38(19)	$\text{N}(9)\text{--Cu}(2)\text{--N}(7')$	91.68(18)
$\text{N}(6)\text{--Cu}(1)\text{--N}(4)$	160.4(2)		

It should be noted that complexes **1** and **4A** have bond lengths and structures that are quite similar. All $\text{Cu}\text{--N}$ distances are very close in both complexes. The $\text{Cu}\text{--N}_{\text{imine}}$ distances are shorter than the $\text{Cu}\text{--N}_{\text{amide}}$ ones in the basal plane and the $\text{Cu}\text{--N}_{\text{pyridine}}$ distances have a value intermediate between them.

Complex **4B** contains the metal atom in a distorted octahedral environment, as in **3**. The copper atom is located on a crystallographic two-fold axis. In this case, both Schiff bases act as monoanionic tridentate N_3 donors, adopting a *mer* disposition. It is remarkable that both Schiff bases are symmetry related in this complex, while they are not in the cobalt analogue nor in $\text{NiL}_3 \cdot 2 \cdot 0.75\text{H}_2\text{O}$.⁵ It should also be noted that the tosyl groups are facing each other, giving rise to weak intramolecular π -stacking interactions. This does not occur in **3**, **4A** nor in the related Ni complex, where the tosyl groups seem to be disposed in order to minimise steric hindrance.

All $\text{Cu}(2)\text{--N}$ distances are in the range of those expected for a hexaco-ordinate copper atom. The $\text{Cu}(2)\text{--N}$ distances [which range from 1.970(5) to 2.264(6) Å] and the $\text{N}\text{--Cu}(2)\text{--N}$ angles [ranging from 76.86(19) to 105.87(18)° and from 154.51(18) to 173.0(3)°] are a result of the deviation from the ideal geometry.

Crystal structure of $\text{ZnL}_3 \cdot 2\text{CH}_3\text{CN}$, **5.** The crystal structure of **5** is shown in Fig. 5 and the main distances and angles in Table 6. The complex consists of discrete mononuclear $\text{ZnL}_3 \cdot 2$ units with lattice acetonitrile. The atoms of one acetonitrile molecule per Zn complex are disordered over two sites, with occupancies of 0.5.

The metal atom can be considered to be in a pentaco-ordinate environment and the structure is closely related to that of complex **4A**. The $\text{Zn}\text{--N}(1)$ bond distance, 2.476(4) Å, is too long to be considered as a true co-ordinated bond, as also occurs in **4A**. However, this distance could be taken as a weak

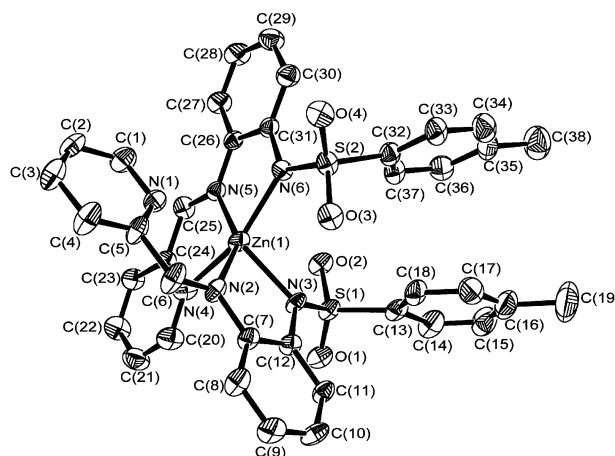


Fig. 5 Molecular crystal structure of $\text{ZnL}_3 \cdot 2\text{CH}_3\text{CN}$, **5**. Ellipsoids are drawn at 50% probability. Acetonitrile solvent is not depicted.

Table 6 Selected bond distances (Å) and angles (°) for **5**

$\text{Zn}(1)\text{--N}(2)$	2.105(4)	$\text{Zn}(1)\text{--N}(6)$	2.094(4)
$\text{Zn}(1)\text{--N}(4)$	2.282(5)	$\text{Zn}(1)\text{--N}(5)$	2.106(4)
$\text{Zn}(1)\text{--N}(3)$	2.087(4)		
$\text{N}(2)\text{--Zn}(1)\text{--N}(3)$	77.81(16)	$\text{N}(3)\text{--Zn}(1)\text{--N}(4)$	89.94(17)
$\text{N}(2)\text{--Zn}(1)\text{--N}(4)$	90.12(16)	$\text{N}(3)\text{--Zn}(1)\text{--N}(6)$	106.01(17)
$\text{N}(2)\text{--Zn}(1)\text{--N}(5)$	147.93(16)	$\text{N}(4)\text{--Zn}(1)\text{--N}(5)$	74.56(16)
$\text{N}(2)\text{--Zn}(1)\text{--N}(6)$	116.23(17)	$\text{N}(4)\text{--Zn}(1)\text{--N}(6)$	151.25(15)
$\text{N}(3)\text{--Zn}(1)\text{--N}(5)$	128.94(16)	$\text{N}(5)\text{--Zn}(1)\text{--N}(6)$	76.83(16)

secondary intramolecular interaction between the metal atom and the pyridine fragment, as previously reported.²⁶

The geometrical parameter τ (with a value of 0.05) indicates square pyramidal geometry around the metal atom, with a distortion of 5% towards a trigonal bipyramid. As in **4A**, the basal positions are occupied by the tridentate $[\text{L}^3]^-$ ligand and by the imine nitrogen atom of the $[\text{L}^3]^-$ bidentate ligand. The amide nitrogen atom of the latter ligand fills the apex of the pyramid. Although both ligands are almost perpendicular (angle between ligands of 88.96°), the tosyl groups are nearly parallel, showing weak intramolecular π -stacking interactions between them, as in **4B**.

The distortion of the complex from ideal geometry is shown by the different Zn–N distances in the basal plane (three of *ca.* 2.1 Å and the fourth of *ca.* 2.28 Å), the short Zn–N_{apical} bond [2.087(4) Å] and the angles around the zinc atom, which range from 74.56(16) to 128.94(16)°. All the distances and angles are very close to the corresponding ones in complex **2**.

A comparison of the four square pyramidal complexes shows some clear patterns. (1) The M–N_{pyridine} bond is always the longest M–N distance for zinc complexes, while it has a value between the M–N_{imine} and M–N_{amide} distance in copper compounds. These latter distances are very similar for the zinc complexes, while they differ significantly in the copper complexes. (2) The distortion of the pyramid in homologous compounds is always higher for the zinc complex. Moreover, the pyramid suffers an elongation in copper compounds, the longer bond being the apical one. The reverse pattern is found for the zinc complexes, where the apical bond length is the shortest of all the Zn–N distances.

IR and ¹H NMR spectroscopy, mass spectrometry and magnetic measurements

IR spectroscopy and mass spectrometry. The IR spectra of all complexes show a broad and strong band at 1585–1603 cm^{-1} , due to the overlap of $\nu(\text{CN}_{\text{imine}})$ and $\nu(\text{CN}_{\text{pyridine}})$. This is indicative of the presence of the Schiff base $[\text{L}^3]^-$ in all the compounds. In addition, two bands in the ranges 1344–1373 and 1125–1133 cm^{-1} are assigned to the asymmetric and symmetric vibration modes of the SO_2 group.²⁷ All the hydrated complexes show a broad band in the range 3400–3500 cm^{-1} , in agreement with the presence of water. No bands above 2500 cm^{-1} were detected in the IR spectra of nonhydrated complexes. This shows that no NH groups are present and therefore that the amide nitrogen atom is deprotonated.

Furthermore, the electrospray MS technique, using methanol solutions, allows the identification of peaks due to the $[\text{ML}^3(p\text{-TosH})]^+$ fragment for complexes of stoichiometry $\text{ML}^3(p\text{-Tos})(\text{H}_2\text{O})_n$ and peaks due to the fragment $[\text{ML}^3_2]^+$ for all $\text{ML}^3_2(\text{H}_2\text{O})_n$ complexes (Table 1), indicating the coordination of the ligands to the metal. Besides, it should be noted that all $\text{ML}^3(p\text{-Tos})(\text{H}_2\text{O})_n$ complexes show also peaks of lower intensity assigned to the $[\text{ML}^3_2]^+$ fragment, suggesting the instability and reorganisation of the initial products in solution.

¹H NMR spectroscopy. The ¹H NMR spectra of both zinc complexes was recorded in DMSO-*d*₆ solvent. However, in spite of the apparent purity of the highly crystalline $\text{ZnL}^3(p\text{-Tos})(\text{H}_2\text{O})_2$ complex, it was not possible to correctly assign all its ¹H NMR signals. This was attributed to the reorganisation of the complex in solution, giving rise to a mixture of products. In fact, most of the signals corresponding to $\text{ZnL}^3_2(\text{H}_2\text{O})$ could be identified. This is also supported by the isolation of the crystallographically characterised $\text{ZnL}^3_2(\text{H}_2\text{O})$, when the DMSO-*d*₆ solution is left to stand. Besides, the intensity of the ¹H NMR signals changes with time, suggesting the coexistence of many species in different proportions.

$\text{ZnL}^3_2(\text{H}_2\text{O})$ shows a different behaviour, generating a clean and unchanging spectrum. Thus, this complex seems to be stable in solution and its ¹H NMR spectrum could be successfully interpreted. In DMSO-*d*₆ it shows one singlet resonance at 9.4 ppm (2H), assigned to the imine protons, indicating the condensation of the amine and the aldehyde. The H_α of the pyridine ring is hidden under a multiplet at 7.9–8.0 ppm as a result of its overlap with the resonances of the aromatic protons, and was located in its ¹H NMR COSY spectrum. The remaining aromatic protons give a triplet signal at 8.08 ppm (2H) and a multiplet signal at 6.76–7.47 (16H). The methyl moiety of the tosyl groups gives a characteristic peak at 2.22 (s, 6H).

Magnetic measurements. Magnetic measurements of all the paramagnetic compounds at room temperature give values for the magnetic moments (Table 1) very close to those expected for magnetically dilute M(II) ions. The magnetic moments of the manganese and copper complexes only allow the oxidation state +2 for the central atom to be confirmed, indicating the deprotonation of the Schiff base ligand. The magnetic moments of $\text{CoL}^3(p\text{-Tos})(\text{H}_2\text{O})_3$ and CoL^3_2 (3.8 and 4.1 BM, respectively) are as expected for high spin cobalt(II) complexes. In the case of CoL^3_2 , the magnetic moment is out of the normal range for Co(II) octahedral complexes (4.7–5.2 BM). This low value implies a small orbital contribution as a consequence of the low symmetry of the complex. This fact could explain the low magnetic moment in the case of $\text{CoL}^3(p\text{-Tos})(\text{H}_2\text{O})_3$. However, in view of the X-ray crystal structures of $\text{ML}^3(p\text{-Tos})(\text{H}_2\text{O})$ (M = Cu, Zn), a square pyramidal geometry could be tentatively proposed. In principle, both structures could be distinguished by UV spectroscopy. Unfortunately, strong charge transfer bands preclude the observation of the d–d transitions.

Conclusions

Electrochemical interaction of L^1 and *p*-TosH with Co, Cu and Zn gives complexes of formula $\text{ML}^3(p\text{-Tos})(\text{H}_2\text{O})_n$. The isolation of these compounds illustrates the instability of the ligand in solution, which undergoes a reorganisation process, preventing the isolation of complexes containing the optically active L^1 as ligand.

$\text{ML}^3_2(\text{H}_2\text{O})_n$ (M = Mn, Co, Cu, Zn) could not be obtained by electrochemical procedures. Instead, chemical template synthesis from Mn(acac)₂, 2-pyridinecarboxaldehyde and *N*-tosyl-1,2-diaminobenzene is a direct general way of obtaining complexes of formula $\text{ML}^3_2(\text{H}_2\text{O})_n$, with high yield and purity.

In addition, the crystallographic characterisation of complexes **1–5** shows that Zn and Cu metals have a preference for the square pyramidal geometry in compounds containing the monoanionic $[\text{L}^3]^-$ ligand.

Experimental

Materials and methods

All solvents, 2-pyridinecarboxaldehyde and the metal acetylacetonates $[\text{Mn}(\text{acac})_2, \text{Co}(\text{acac})_2, \text{Cu}(\text{acac})_2$ and $\text{Zn}(\text{acac})_2]$ were commercial products and were used without further purification. Manganese, cobalt, copper and zinc (Ega Chemie) were used as *ca.* 2 × 2 cm^2 plates. *N*-Tosyl-1,2-diaminobenzene was obtained as previously reported by Malik and Sharma.²⁸

L^1 and L^2 were obtained as previously described⁵ and characterised by elemental analysis, melting point, IR, mass and ¹H NMR spectra.

Elemental analyses were performed on a Carlo Erba EA 1108 analyser. NMR spectra were recorded on a Bruker AC-300 spectrometer using DMSO-*d*₆ solvent. Infrared

spectra were recorded from KBr pellets on a Bio-Rad FTS 135 spectrophotometer in the range 4000–600 cm^{-1} . Electro-spray mass spectra were obtained on a Hewlett-Packard LC/MS spectrometer, in methanol as solvent. Room temperature magnetic measurements were performed using a Sherwood Scientific magnetic susceptibility balance, calibrated using mercury tetrakis(isothiocyanato)cobaltate(II).

Synthesis of the complexes

$\text{ML}^3(p\text{-Tos})(\text{H}_2\text{O})_n$. These were obtained using an electrochemical procedure, exemplified by the isolation of $\text{CuL}^3(p\text{-Tos})(\text{H}_2\text{O})$, **1**. An acetonitrile solution (70 mL) of L^1 (0.2 g, 0.41 mmol) and *p*-toluenesulfonic acid (0.14 g, 0.82 mmol), containing about 10 mg of tetramethylammonium perchlorate supporting electrolyte, was electrolysed for about 2 h using a current of 10 mA. A platinum wire was used as the cathode and a copper plate as the anode. The resulting suspension was filtered, yielding the brown solid $\text{CuL}^3(p\text{-Tos})(\text{H}_2\text{O})_3$. The mother liquors were left to stand for one week. Evaporation of the solution yielded small green crystals of $\text{CuL}^3(p\text{-Tos})(\text{H}_2\text{O})$, **1**, suitable for X-ray diffraction studies. Crystals of $\text{ZnL}^3(p\text{-Tos})(\text{H}_2\text{O})$, **2**, were obtained in exactly the same way, using a zinc plate as the anode.

A grey solid of empirical formula $\text{Mn}(p\text{-Tos})_2(\text{H}_2\text{O})_6$ was obtained by the same method, using manganese as the anode: m.p. $>300^\circ\text{C}$; anal. found (calc.) for $\text{MnC}_{14}\text{H}_{26}\text{O}_{12}\text{S}_2$: C: 32.9 (33.3); H: 5.5 (5.1); N: 0 (0); S: 13.3 (12.7)%.

Slow recrystallisation of $\text{CoL}^3(p\text{-Tos})(\text{H}_2\text{O})_3$ in CH_3CN yielded crystals of $\text{Co}(p\text{-Tos})_2(\text{H}_2\text{O})_6$: m.p. $>300^\circ\text{C}$; anal. found (calc.) for $\text{CoC}_{14}\text{H}_{26}\text{O}_{12}\text{S}_2$: C: 33.7 (33.0); H: 5.4 (5.1); N: 0 (0); S: 13.6 (12.6)%. Unit cell: $a = 6.9867(1)$; $b = 6.3049(1)$; $c = 25.2330(1)$ Å; $\beta = 91.7544(8)^\circ$.

$\text{ZnL}^3_2(\text{H}_2\text{O})$. This complex was isolated by two different methods. *Method A* (electrochemical synthesis): To an acetonitrile solution (70 mL) of L^2 (0.2 g, 0.57 mmol), 10 mg of tetramethylammonium perchlorate were added as supporting electrolyte. The resulting solution was electrolysed for 1.5 h with a current of 10 mA, using a platinum wire as the cathode and a zinc plate as the anode. During the experiment, an orange solid precipitated. The solid was isolated by filtration, washed with diethyl ether and dried in air.

Method B (chemical template synthesis): To a methanol solution (80 mL) of $\text{Zn}(\text{acac})_2$ (0.25 g, 0.95 mmol), 2-pyridinecarboxaldehyde (0.18 mL, 1.9 mmol) and *N*-tosyl-1,2-diaminobenzene (0.5 g, 1.9 mmol) were added. The mixture was refluxed for 3 h, removing the water with a Dean–Stark device. The resultant suspension was filtered and the orange solid was washed with diethyl ether and dried in air. Recrystallisation of the orange powder in hot acetonitrile yielded crystals of $\text{ZnL}^3_2 \cdot 2\text{CH}_3\text{CN}$, **5**, suitable for X-ray diffraction studies. ^1H NMR in $\text{DMSO}-d_6$: δ 9.4 (s, 2H, CH=N), 8.08 (t, 2H, H_{arom}); 7.9–8.0 (m, 6H, $4\text{H}_{\text{arom}} + 2\text{H}_{\text{pyridine}}$) 6.76–7.47 (m, 16H, H_{arom}), 2.22 (s, 6H, methyl).

$\text{ML}^3_2(\text{H}_2\text{O})_n$. All $\text{ML}^3_2(\text{H}_2\text{O})_n$ complexes (M = Mn, Co, Cu, Zn) can be obtained by method B. Recrystallisation of the dark brown solid CoL^3_2 in CH_3CN and of the dark red powder CuL^3_2 , by slow evaporation of a methanol–ethanol–dichloromethane solution, yielded crystals of CoL^3_2 , **3**, and CuL^3_2 , **4**, respectively, suitable for X-ray diffraction studies.

CoL^3_2 . This complex has also been obtained by two different procedures: chemical template synthesis (method B above) and by an electrochemical template synthesis: To an acetonitrile solution (70 mL) of *N*-tosyl-1,2-diaminobenzene (0.2 g, 0.76 mmol) and 2-pyridinecarboxaldehyde (0.8 mL, 0.8 mmol), 10 mg of tetramethylammonium perchlorate were added as supporting electrolyte. The resultant solution was electrolysed for 2 h with a current of 10 mA, using a platinum wire as the

cathode and a cobalt plate as the anode. The garnet solution was reduced in volume and the precipitated solid isolated by filtration, washed with diethyl ether and dried in air.

Crystallographic measurements

Crystal structures of $\text{CuL}^3(p\text{-Tos})(\text{H}_2\text{O})$, **1 and $\text{ZnL}^3(p\text{-Tos})(\text{H}_2\text{O})$, **2**.** Crystals suitable for single X-ray diffraction studies of **1** and **2** were obtained as previously described. Data were collected at 293 K using a CAD-4 diffractometer employing graphite-monochromated $\text{Mo-K}\alpha$ ($\lambda = 0.71073$ Å) radiation, using the $\omega/2\theta$ scan mode ($2\theta_{\text{max}} = 55.94^\circ$ for **1** and 49.98° for **2**). The structures were solved by direct methods and refined by full matrix least squares on F^2 . All hydrogen atoms were included in calculated positions, except those attached to oxygen atoms, which were located in the Fourier map and isotropically refined. Data processing and computation were carried out using the SHELX-97 program package.²⁹

Crystal structure of CoL^3_2 , **3.** Brown plate crystals of **3** were obtained as described above. All measurements were made at 293(2) K on a Smart-CCD-1000 Bruker diffractometer employing $\text{Mo-K}\alpha$ ($\lambda = 0.71073$ Å) radiation, using the ω scan mode ($2\theta_{\text{max}} = 52.98^\circ$). An absorption correction from ψ scans was applied. The structure was solved by direct methods and refined by full matrix least squares on F^2 . Non-hydrogen atoms were refined anisotropically. All hydrogen atoms were included in calculated positions. Data processing and computation were carried out using the SHELX-97 program package.²⁹

Crystal structures of CuL^3_2 , **4 and $\text{ZnL}^3_2 \cdot 2\text{CH}_3\text{CN}$, **5**.** Block-like dark red and orange plate crystals of **4** and **5**, respectively, were obtained as detailed above. All measurements were made at 293(2) K on a Rigaku AFC5R diffractometer for **4** and on a Siemens CCD diffractometer for **5**, employing $\text{Mo-K}\alpha$ ($\lambda = 0.71073$ Å) radiation, using the 2θ scan mode ($2\theta_{\text{max}} = 56.56^\circ$ for **4** and 49.94° for **5**). The structures were solved by direct methods and refined by full matrix least squares on F^2 . Non-hydrogen atoms were refined anisotropically. All hydrogen atoms were included in calculated positions. Data processing and computation were carried out using the SHELX-97 program package.²⁹

CCDC reference numbers 153998–154002. See <http://www.rsc.org/suppdata/nj/b0/b008932j/> for crystallographic data in CIF or other electronic format.

Acknowledgements

The authors would like to thank the Ministerio de Educación y Ciencia (Spain) (PB98-0600) and Xunta de Galicia (Spain) (PGIDT00PXI20910PR) for financial support.

References

- D. A. Garnovskii, A. L. Nivorozhkin and V. I. Minkin, *Coord. Chem. Rev.*, 1993, **126**, 1.
- V. Alexander, *Chem. Rev.*, 1995, **95**, 273.
- S. Yamada, *Coord. Chem. Rev.*, 1999, **190–192**, 537.
- (a) M. Watkinson, M. Fondo, M. R. Bermejo, A. Sousa, C. A. McAuliffe, R. G. Pritchard, N. Jaiboon, N. Aurangzeb and M. Naeem, *J. Chem. Soc., Dalton Trans.*, 1999, 31 and references therein; (b) M. Maneiro, M. R. Bermejo, A. Sousa, M. Fondo, A. M. González, A. Sousa-Pedrares and C. A. McAuliffe, *Polyhedron*, 2000, **19**, 47.
- M. R. Bermejo, A. Sousa, M. Fondo and M. Helliwell, *New J. Chem.*, 2000, **24**, 33.
- S. Cabaleiro-Martónez, J. Castro, J. Romero, J. A. García-Vázquez and A. Sousa, *Acta Crystallogr., Sect. C*, 2000, **56**, E249.
- A. W. Addison, T. N. Rao, J. Reedijk, J. Van Rijk and C. G. Verschoor, *J. Chem. Soc., Dalton Trans.*, 1984, 1349.
- A. Jäntti, K. Rissanen and J. Valkonen, *Acta Chem. Scand.*, 1998, **52**, 1010.

- 9 N. V. Gerbelen, A. D. Garnovskii, V. B. Arion, P. N. Bourosh, Y. A. Simonov, V. A. Alekseenko, K. M. Indrichan and A. V. Khokhlov, *Russ. J. Inorg. Chem.*, 1988, **33**, 1013.
- 10 M. L. Durán, J. A. García-Vázquez, J. Romero, A. Castiñeiras, A. Sousa, A. D. Garnovskii and D. A. Garnovskii, *Polyhedron*, 1997, **16**, 1707.
- 11 A. D. Garnovskii, A. S. Burlov, D. A. Garnovskii, I. S. Vasilchenko, A. S. Antsichkina, G. S. Sadikov, A. Sousa, J. A. García-Vázquez, J. Romero, M. L. Durán, A. Sousa-Pedrares and C. Gómez, *Polyhedron*, 1999, **18**, 863.
- 12 C. Chieh and G. P. Palenik, *Inorg. Chem.*, 1972, **11**, 816.
- 13 Z. He, P. J. Chaimungkalanont, D. C. Craig and S. B. Colbran, *J. Chem. Soc., Dalton Trans.*, 2000, 1419.
- 14 T. Koike, E. Kimura, I. Nakamura, Y. Hashimoto and M. Shiro, *J. Am. Chem. Soc.*, 1992, **114**, 7338.
- 15 J. Romero, J. A. García-Vázquez, M. L. Durán, A. Castiñeiras, A. Sousa, A. D. Garnovskii and D. A. Garnovskii, *Acta Chem. Scand.*, 1997, **51**, 672.
- 16 E. Amadei, M. Carcelli, S. Ianelli, P. Cozzini, P. Pelagatti and C. Pelizzi, *J. Chem. Soc., Dalton Trans.*, 1998, 1025.
- 17 S. Ianelli, G. Minardi, C. Pelizzi, G. Pelizzi, L. Reverberi, C. Solinas and P. Tarasconi, *J. Chem. Soc., Dalton Trans.*, 1991, 2113.
- 18 A. Bino and N. Cohen, *Inorg. Chim. Acta*, 1993, **210**, 11.
- 19 D. Wester and G. J. Palenik, *Inorg. Chem.*, 1976, **15**, 755.
- 20 C. Bolos, P. C. Christidis, G. Will and L. Wiehl, *Inorg. Chim. Acta*, 1996, **248**, 209.
- 21 I. Ivanovic-Burmazovic, A. Bacchi, G. Pelizzi, V. M. Leovac and K. Andjelkovic, *Polyhedron*, 1999, **18**, 119.
- 22 F. Hueso-Ureña, N. A. Illán-Cabeza, M. N. Moreno-Carretero, A. L. Peñas-Chamorro and R. Faure, *Polyhedron*, 2000, **19**, 689.
- 23 D. Wester and G. J. Palenik, *J. Am. Chem. Soc.*, 1975, **96**, 7565.
- 24 R. A. D. Wentworth, P. S. Dahl, C. J. Huffman, W. O. Gillum, W. E. Streib and J. C. Huffman, *Inorg. Chem.*, 1982, **21**, 3060.
- 25 G. Bomberl, E. Forsellini, A. Del Para, M. L. Tobe, C. Chattrjee and C. Cooksey, *Inorg. Chim. Acta*, 1983, **75**, 93.
- 26 A. D. Garnovskii, A. S. Antsishkina, I. S. Vasilchenko, V. S. Sergienko, S. G. Kochin, A. L. Nirovzorkhin, A. E. Mistryukov, A. E. Uraev and D. A. Garnovskii, *Russ. J. Inorg. Chem.*, 1995, **40**, 67.
- 27 M. Morioka, M. Kato, H. Yoshida and T. Ogata, *Heterocycles*, 1997, **45**, 1173.
- 28 W. U. Malik and T. S. Sharma, *J. Indian Chem. Soc.*, 1970, **47**, 167.
- 29 G. M. Sheldrick, SHELX97, Programs for Crystal Structure Analysis, Institut für Anorganische Chemie der Universität, Göttingen, Germany, 1998.